

Estimating System State During Human Walking with a Powered Ankle-Foot Orthosis

Yifan Li, *Member, IEEE, ASME*, Aaron Becker, *Member, IEEE*, K. Alex Shorter, Timothy Bretl, *Member, IEEE*, Elizabeth T. Hsiao-Weckslar, *Member, IEEE, ASME*

Abstract—This paper presents a state estimator that reliably detects gait events during human walking with a portable powered ankle-foot orthosis (AFO), based only on measurements of the ankle angle and of contact forces at the toe and heel. Effective control of the AFO critically depends on detecting these gait events. A common approach detects gait events simply by checking if each measurement exceeds a given threshold. Our approach uses cross-correlation between a window of past measurements and a learned model to estimate the configuration of the human walker, and detects gait events based on this estimate. We tested our approach in experiments with five healthy subjects and with one subject that had neuromuscular impairment. Using motion capture data for reference, we compared our approach to one based on thresholding and to another common one based on k -nearest neighbors. The results showed that our approach reduced the RMS error by up to 40% for the impaired subject and up to 49% for the healthy subjects. Moreover, our approach was robust to perturbations due to changes in walking speed and to control actuation.

Index Terms—Gait, State Estimation, Cross-correlation, Event Detection, AFO

I. INTRODUCTION

GAIT is a cyclic task characterized by repetitive events, and is defined from the initial ground contact of the foot to the subsequent contact of the same foot. Gait events are used to divide the cycle into phases and subphases each with a functional objective that contributes to one of three main functional tasks during gait: weight acceptance (stance), support and propulsion (stance), and limb advancement (swing) [1]–[3]. Gait can be impaired by conditions including trauma, incomplete spinal cord injuries, stroke, multiple sclerosis, muscular dystrophies, polio or cerebral palsy [1]. These deficiencies create impairments because they prevent or hinder the functional tasks required for gait.

Ankle-foot orthoses (AFOs) are orthotic devices used to correct gait deficiencies created by impairments to the lower limbs. In the United States alone, sizable populations exist with symptoms that can be treated with an AFO: stroke (4.7M), polio (1M), multiple sclerosis (400K), spinal cord injuries (200K) and cerebral palsy (100K) [4]. Clinically prescribed AFO systems assist impaired individuals by providing

support for the lower leg and foot while restricting unwanted motion of the foot in a predetermined and fixed manner [5]–[8]. Unfortunately, these fixed motion control properties can impede gait and cannot adapt to a changing environment [9]. Powered AFO systems address the limitations of passive devices by using computer control to vary the compliance, damping, or net power of the device for motion control and torque assistance at the ankle joint [9]–[12].

The performance of a powered AFO depends critically on the ability to do two things: first, detect gait events based on measurements from onboard sensors (e.g., accelerometers, potentiometers, and force sensors), and second, control applied torque to meet the functional objective determined by each gait event. Our focus in this paper is on the first of these things, reliable detection of gait events.

Many state-of-the-art AFOs detect gait events simply by checking if each sensor measurement at a particular time exceeds a given threshold [9]–[18]. This approach has been used to provide appropriately timed motion control and torque assistance both for level walking and for stair climbing. However, this approach becomes less reliable when the individual’s gait pattern changes, for example as the result of impairment, fatigue, preference, or functional assistance from the orthosis. Moreover, this approach may not even be possible when there exists no unambiguous mapping from sensor measurements to a gait event of interest, in particular an event other than “heel-strike” or “toe-off.” These situations limit the number and reliability of gait events that can be used for control.

In this paper we consider an alternative approach that uses the time history of sensor measurements to compute an estimate of body configuration and then detects gait events based on this estimate. It is well known that body configuration during cyclic gait can be approximated by a single state variable, the “percent gait cycle,” and that gait events are associated with particular values of this state variable [1]. Recent work has shown that it is possible to compute an estimate of this state variable by comparing motion capture data (producing measurements of lower-limb joint angles and joint velocities) to a learned model [19]. We will do the same, but must address the fact that a powered AFO typically does not have access to motion capture data, nor to similarly rich sensor measurements.

In particular, our approach computes a state estimate (i.e., an estimate of where an individual is in the gait cycle) based only on measurements of the ankle angle and of contact forces at the toe and heel. These measurements are taken only from sensors mounted on the portable powered AFO (PPAFO)

Y. Li, K. A. Shorter, and E. T. Hsiao-Weckslar are the Department of Mechanical Science and Engineering, University of Illinois at Urbana Champaign, Urbana, IL, 61820 USA email: {yifanli4,shorter2,ethw}@illinois.edu

A. Becker is with the Department of Electrical and Computer Engineering, University of Illinois at Urbana Champaign, email: abecker5@illinois.edu

T. Bretl is with the Department of Aerospace Engineering, University of Illinois at Urbana Champaign, email: tbretl@illinois.edu

Manuscript received November 1, 2010

that we use in our experiments [18]. This sensor package is comparable to what is found on other AFOs, including those of Blaya and Herr [10] with joint angle and ground reaction force sensors, Svensson and Holmberg [9] with a joint angle sensor, and Hollander et al. [15] with a joint angle sensor and foot switches. None of these sensor packages are sufficient to compute a state estimate based only on one set of measurements. However, due to the cyclic nature of gait, sensor measurements from different gait cycles exhibit a high degree of correlation. We take advantage of this fact to compute a state estimate based on maximizing the cross-correlation between a window of past sensor measurements and a reference model learned from training data. When tested in experiments with human subjects, our approach to event detection was more accurate and more robust to changes in gait than other approaches previously reported in the literature.

A. Overview

Throughout this paper, we will denote time by $t \in \mathbb{R}$, the state variable describing percent gait cycle by $\lambda \in [0, 100)$, and the vector of sensor measurements by $\mathbf{y} \in \mathbb{R}^3$. Since the mapping from λ to gait events is well known [1], our goal is to compute an estimate $\hat{\lambda}(t)$ of the state $\lambda(t)$ at the current time t based on all sensor measurements $\{\mathbf{y}(s) | s \in [0, t]\}$ up to this time. In our experiments, we use the method of [19] to compute a reference estimate $\lambda^*(t)$ based on motion capture data, and define the error in our own estimate by

$$\lambda_{\text{err}}(t) = \hat{\lambda}(t) - \lambda^*(t).$$

To examine the performance of our proposed cross-correlation estimator, we compare it to two other estimators and to a direct event detector. All three estimators that we consider are based on a precomputed model $\bar{\mathbf{y}}(\lambda)$ that tells us what sensor measurements to expect at a given state λ . This model is given by regression analysis of training data (λ^*, \mathbf{y}) . We also derive the average cycle period T from this model. The estimators and direct event detector are as follows:

- **Cross-Correlation (CC)** The estimate $\hat{\lambda}_{\text{CC}}$ minimizes the sum-squared-error between sensor readings from the last T seconds and training data with a phase shift of $\hat{\lambda}_{\text{CC}}$.
- **k -Nearest-Neighbors ($k\text{NN}$)** The estimate $\hat{\lambda}_{k\text{NN}}$ minimizes the squared-error between the current sensor reading and training data at $\hat{\lambda}_{k\text{NN}}$.
- **Fractional-Time (FT)** The estimate $\hat{\lambda}_{\text{FT}}$ is the time since the last heel strike (determined by thresholding the heel sensor) normalized by T .
- **Direct Event (DE)** DE uses thresholds on heel and toe sensors to determine heel strike and toe off events. Because DE is limited to these two events, it is not a state estimator.

FT is similar to what is found in the AFO literature [9]–[18], $k\text{NN}$ is similar to [19] but applied to AFO sensor data rather than motion capture data, and CC is the approach that we present here. We emphasize that cross-correlation is a classical method of signal processing (e.g., [20]) that has been used previously for gait analysis (e.g., [21], [22]). Our contribution is the application of this approach to state estimation for a

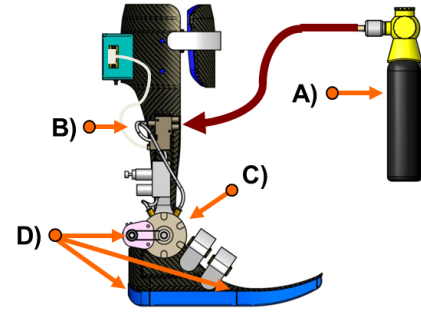


Fig. 1. PPAFO system components: A) Power supply: a compressed CO_2 bottle with regulator provides up to 120psi for the system; B) Valves: two 3-2 solenoid valves control the flow of CO_2 to the actuator; C) Actuator: a pneumatic rotary actuator provides up to 12Nm at 120psi; D) Sensors: two force sensors under the heel and toe, and a potentiometer at the ankle joint.

powered AFO and the analysis of experiments with human subjects necessary to demonstrate its performance.

The remainder of our paper proceeds as follows. Section II describes the experimental methods used to quantify the performance of each state estimator. Section III presents the details of our CC state estimator and two others used as a basis for comparison. Section IV provides the results of experiments with five healthy subjects and one subject that had neuromuscular impairment. Section V considers the implications of these results in the context of AFO control. Section VI gives concluding remarks.

II. EXPERIMENTAL METHODS

Three state estimators (CC, $k\text{NN}$, and FT) and DE were implemented on a powered AFO capable of operation in real-world environments outside of the laboratory or clinic. A reference estimate λ^* was also derived using kinematic data from a motion capture system and kinetic data from an instrumented treadmill. Experimental trials with five healthy subjects and one subject with a neuromuscular impairment were performed to assess the three AFO estimators on their performance relative to the reference state model λ^* , ability to identify relevant gait events during the cycle, and robustness to speed and actuation perturbations. This section describes the PPAFO system, the gait lab data collection procedure, and the experimental setup.

A. Powered Orthosis System

The PPAFO in this work used a pneumatic power supply and a rotary actuator at the AFO ankle joint for motion control and propulsion assistance, Figure 1, [18]. The PPAFO control loop and estimators ran at 66Hz, using sensor feedback sampled at the same rate from two force sensors (0.5in circle, Interlink Electronics, Camarillo, CA) mounted underneath the heel and toe between the carbon fiber shell and the sole of the PPAFO and a potentiometer (53 Series, Honeywell, Golden Valley) that measured the angle between the shank and foot sections.

B. Experimental Setup and Pre-Test Procedures

1) *Experimental Setup*: Subjects walked with the PPAFO on an instrumented treadmill. For each trial, the subject wore sleeveless top and snug-fitting shorts. Thirty-two reflective markers were attached to the body, including torso, thighs, shanks, feet and the PPAFO. Data from the healthy subject were collected at the University of Illinois. Kinematic data were collected using a 6-camera motion capture system sampled at 150Hz (Model 460; Vicon, Oxford, UK). Ground reaction force (GRF) data for each foot was collected on a split-belt treadmill with embedded force plates sampled at 1500Hz (Bertec, Columbus, OH, USA). Data from the impaired subject were collected at Georgia Institute of Technology. Kinematic data were collected using a 6-camera system sampled at 120Hz (Model 460; Vicon, Oxford, UK). The kinetic data were collected on a custom force-sensing instrumented split-belt treadmill sampled at 1080Hz [23]. Joint angles were calculated from kinematic data. Joint angles and GRF were filtered by a low-pass, fourth-order, zero-lag, Butterworth filter with cut-off frequency of 10Hz. All procedures were approved by the institutional review boards of the University of Illinois and Georgia Institute of Technology, and all participants gave informed consent.

2) Subject Information:

a) *Healthy Subjects*: The five healthy male subjects (28±4yrs; height 186±5cm; mass 72±8kg) had no gait impairments and no history of significant trauma to the lower extremities or joints.

b) *Impaired Subject*: The impaired male subject (51yrs; height 175cm; mass 86kg) has a diagnosis of *cauda equina syndrome* (CES) caused by a spinal disc rupture. This gait deficit does not allow him to generate plantarflexor torque to push his toes down. The subject walks without the use of walking aids (i.e., cane or walker), but usually wears AFOs bilaterally. For our testing, he wore his own pre-fabricated carbon composite AFO (Blue Rocker™, Allard, NJ, USA) on his left leg while walking with the PPAFO on his right leg.

3) *Determining Self-Selected Speed*: A self-selected walking speed for each subject was determined prior to testing. For the healthy subjects, comfortable treadmill walking speed was determined by averaging three self-selected speeds chosen while wearing the PPAFO with no actuation. Average walking speed for the five healthy subjects was 1.18±0.11m/s with an average gait period of 1.16±0.09s over 30 seconds of walking. The impaired subject's comfortable walking speed was determined while in his running shoes on the treadmill with no assistive devices on either leg. This walking condition was used because it was the impaired subject's most difficult condition. Walking speed for the impaired subject was 0.7m/s with an average gait period of 1.09±0.04s over 30 seconds of walking.

C. Training Data for Estimation Models

The PPAFO state estimators require a model derived from data collected during a preliminary training process. Each model is unique to each subject, and is not varied between experimental trials. During this process, a subject walked

with the unactuated PPAFO on the treadmill for 30s at his comfortable walking speed.

GRF_Z data from the force-sensing treadmill were compared to a threshold to identify heel strikes. The average period of the gait cycle, T , was calculated from these data.

The data were also used to create regression models for each of the PPAFO sensor measurements during gait cycles. Models for different sensors were computed separately. Each model is a function of cycle state λ , where $\lambda \in [0, 100)$, and describes the expected reading for a given sensor $\bar{y}(\lambda)$. The regression models were formulated in the following manner.

For each sensor, we use locally weighted regression (LWR) analysis [24] to establish the functional relationship between the normalized input/output pairs of state λ and sensor measurement y .

$$(\lambda_1, y_1), \dots, (\lambda_N, y_N),$$

where N is the number of measurements collected from training, and λ is the percent gait cycle found by normalizing time between heel strikes.

Regression evaluates \bar{y} at the point λ . This evaluation depends on the signed distance

$$x_i = \text{dist}(\lambda_i - \lambda)$$

between λ_i and the query point λ . Because λ_i and $\lambda \in [0, 100)$, the distance is defined as

$$\text{dist}(\lambda_i - \lambda) = \begin{cases} (\lambda_i - \lambda) - 100 & \text{if } \lambda_i - \lambda > 50 \\ \lambda_i - \lambda & \text{if } -50 \leq \lambda_i - \lambda \leq 50 \\ (\lambda_i - \lambda) + 100 & \text{if } \lambda_i - \lambda < -50 \end{cases}$$

First, we select a fixed set of M polynomial basis functions

$$\phi(x_i) = [1, x_i, \dots, x_i^{M-1}]^T,$$

and denote

$$\Phi = \begin{bmatrix} \phi(x_1)^T \\ \vdots \\ \phi(x_N)^T \end{bmatrix}.$$

We also define

$$Y = \begin{bmatrix} y_1 \\ \vdots \\ y_N \end{bmatrix}$$

by concatenating the data associated with each output. We select the row vector $v \in \mathbb{R}^M$ of parameters that minimizes the weighted sum-squared error e

$$e = \sum_{i=1}^N w_i (y_i - v^T \phi(x_i))^2$$

where

$$w_i = \exp\left(-\frac{x_i^2}{2r^2}\right) \text{ for each } i = 1, \dots, N$$

and r is a design parameter. Because w_i depends explicitly on λ , we must store and use the entire set of training data $(\lambda_1, y_1), \dots, (\lambda_N, y_N)$ to make predictions. Let

$$W = \text{diag}(w_1, \dots, w_N)$$

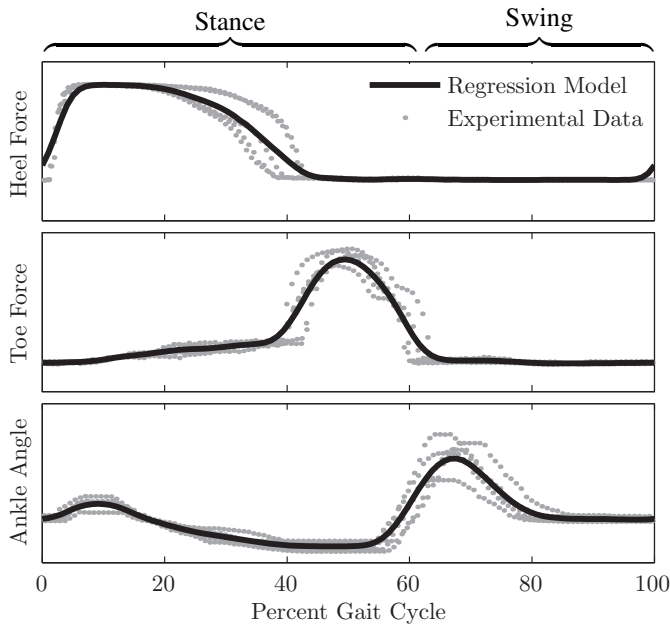


Fig. 2. Locally-weighted linear regression analysis with $M = 2$ polynomial basis functions and a weighting bandwidth of $r = 0.02$ applied to heel force, toe force and ankle angle sensor measurements as a function of percent gait cycle. 5 cycles of sensor measurements (gray dots) from healthy subject #3 walking at steady-state, self-selected speed were used to create a regression model $\bar{y}(\lambda)$, shown in black, for each sensor.

then the cost function can be rewritten in matrix form

$$e = (\Phi v - Y)^T W (\Phi v - Y).$$

In order to minimize e , v can be solved as

$$v(\lambda) = (\Phi^T W \Phi)^{-1} \Phi^T W Y$$

Now we can obtain the regression model for a given sensor over one gait cycle as

$$\bar{y}(\lambda) = v(\lambda)^T \phi(0)$$

For each subject, we precompute $\bar{y}(\lambda)$ at $\lambda = \{0, 1, \dots, 99\}$ for all three sensors, and they will form the sensors regression model matrix $\bar{y}(\lambda)$. The results of applying this form of regression analysis to multiple gait cycles of healthy subject #3 are shown in Fig. 2.

D. Experimental Testing Procedure

Tests were conducted with two possible disturbances: *actuation* and *slow speed*. The actuation disturbance modeled the effect of providing assistive torque with the PPAFO. During each gait cycle, a plantarflexor (toes down) disturbance torque was applied if both the toe and heel sensors were loaded, and a dorsiflexor (toes up) disturbance torque was applied if both sensors were unloaded—otherwise, no disturbance torque was applied. State estimates (from CC, k NN, or FT) could also have been used to trigger the application of torque in these experiments, but the use of a simple decision rule allowed for a less biased comparison between estimators. Figure 3 shows the resulting change in gait kinematics as a consequence of actuation. The slow speed disturbance modeled the effect of

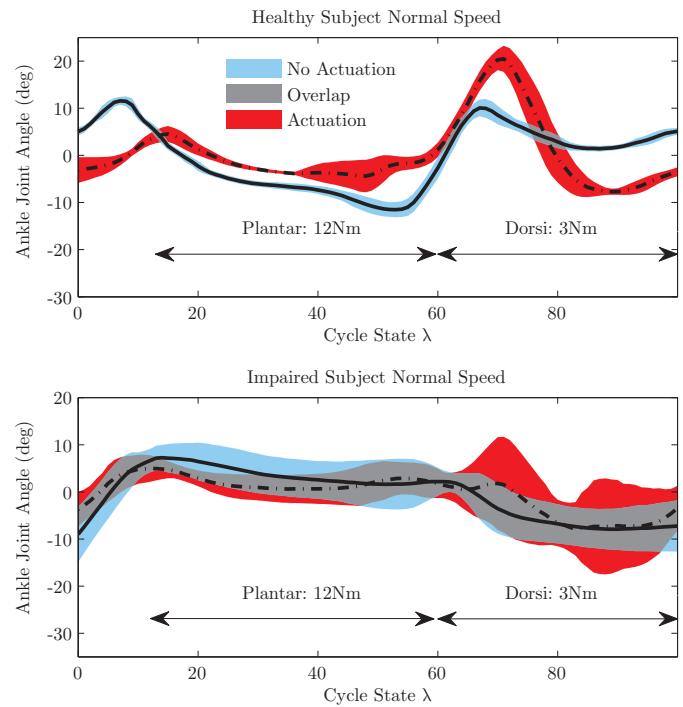


Fig. 3. Ankle joint angle for healthy subject #3 (top) and the impaired subject (bottom) with and without actuation at normal speed. The PPAFO was able to generate a modest plantarflexor torque (12Nm) compared to a healthy walker (105Nm for a 70kg individual). Only 3Nm of dorsiflexor torque was required to support the foot during swing. Sensor readings without actuation and with actuation are significantly different. Because the sensor regression model was generated without actuation, these differences resulted in worse correlation between current measurements and the model. For the impaired subject, excessive dorsiflexion actuation during swing may have caused the large variability of ankle joint position.

variable walking speed, which is a common gait perturbation. It was created by slowing the treadmill.

Five experimental trials were used to evaluate the performance of the PPAFO estimators under these two disturbances. For each test, the subjects were given time to reach a steady walking speed on the treadmill before data collection began. Thirty seconds of data were recorded during steady-state walking for trials 1-4.

1) *Normal Speed – No Actuation (Healthy and Impaired)*: This test compares the PPAFO estimators under nominal conditions. Each subject walked at his self-selected speed (normal speed) with no actuation from the PPAFO.

2) *Normal Speed – Actuation (Healthy and Impaired)*: Torque applied by the PPAFO can affect gait timing and sensor readings, adversely impacting estimation. The PPAFO was supplied with pneumatic power at 110psi and actuated by the simple threshold rule described above.

3) *Slow Speed – No Actuation (Healthy and Impaired)*: The treadmill was set to 75% of the subject's self-selected speed, with no PPAFO actuation.

4) *Slow Speed – Actuation (Healthy and Impaired)*: This trial examined the effects of slow walking (75% of self-selected speed) along with actuation. The actuation was in the same manner as trial 2 above.

5) **Change in Speed (Healthy)**: Changing speed is a common gait perturbation. A speed change was introduced to examine the effect of this perturbation on the accuracy of the PPAFO estimators. Each healthy subject began walking at his self-selected speed. After 20s, the treadmill was gradually slowed to 75% of self-selected speed in approximately 5s. The speed remained 75% of self-selected speed for the rest of the trial. Sixty seconds of data were recorded during the trial.

E. Estimation Comparison Metrics

Two metrics were used to evaluate and compare the performance of the PPAFO estimators for the tests in section II-D:

- 1) **Event Detection**: Temporal errors were compared between gait event times identified using gait lab data, event times predicted by the three PPAFO estimators, the direct event detector, and the reference state estimator λ^* . The gait events selected for comparison were right heel strike, left toe off, left heel strike and right toe off.
- 2) **State Estimation**: Errors were compared between reference state estimate λ^* and the three PPAFO state estimates throughout the cycle.

III. STATE ESTIMATION TECHNIQUES

The experiments described in the previous section tested three state estimators (CC, FT, and k NN) and the direct event detector (DE), all based on PPAFO sensor measurements in comparison to a reference estimate (λ^*) based on motion capture and treadmill data. In this section we will describe how each state estimator was implemented.

A. Estimate Based on Cross-Correlation (CC)

The CC estimator slides a window of actual sensor data across the regression model of the sensor data, and finds the point where the mean-square-error is minimized (i.e., where the data and model best align). Given the regression model \bar{y} and the average period T , we can apply the CC approach to estimate λ at each time t . We do this in the following way. We have precomputed $\bar{y}[\lambda]$ at $\lambda = \{0, 1, \dots, 99\}$ using the locally weighted linear regression approach mentioned above. We take a time-history of sensor data $\mathbf{y}_1, \dots, \mathbf{y}_m$ sampled at m particular times $t_1, \dots, t_m \in [t-T, t]$. For all $j = 1, \dots, m$, we normalize these times according to

$$\lambda_j = 100 \left(\frac{t_j - (t - T)}{T} \right),$$

then generate an index set $I = I_1, \dots, I_m$ according to

$$I_j = \text{round}(\lambda_j),$$

so that each I_j will be an integer index between 0 and 100. We denote the measurements by $\mathbf{y}[j] = \mathbf{y}_j$. We wrap the regression model around periodic borders by setting $\bar{y}[i] = \bar{y}[i \pm 100]$ for all i . The state estimate $\hat{\lambda}_{CC}$ is the integer $k \in \{0, \dots, 99\}$ that minimizes

$$\sum_{j=1}^m (\bar{y}[I_j + k] - \mathbf{y}[j])^T (\bar{y}[I_j + k] - \mathbf{y}[j]).$$

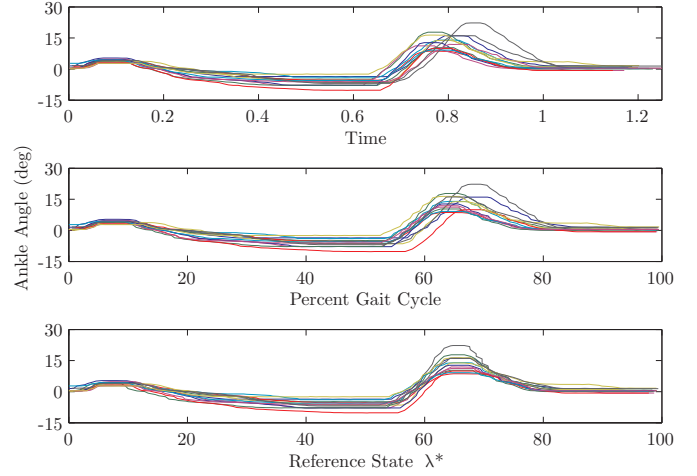


Fig. 4. The ankle angles of healthy subject #3 aligned at heel strike for ten cycles. The angle is plotted with respect to time, percent gait cycle, and reference estimate λ^* .

B. Estimate Based on Fractional Time (FT)

The fractional time (FT) estimator assumes that the state estimate $\hat{\lambda}$ increases linearly with time from heel-strike:

$$\hat{\lambda}_{FT} = 100(t - t_{hs})/T,$$

where t_{hs} is the time of last heel strike as determined by thresholding $y(t_{hs})$, and T is the average cycle period.

C. Estimate Based on k -Nearest Neighbor (k NN)

Another common way to estimate state is to compute the best match between current sensor measurements \mathbf{y} and the regression model learned from training data \bar{y} :

$$\hat{\lambda}_{kNN} = \arg \min_{\lambda \in [0, 100]} \|\mathbf{y}(t) - \bar{y}(\lambda)\|_2$$

This approach can be improved by averaging the k best matches (" **k nearest neighbors**" [25]). We chose $k = 3$.

D. Reference Estimate (λ^*)

We use an estimator generated from motion capture and treadmill data as a reference for comparing the PPAFO estimators. The joint angle information expands 8 variables (vertical ground reaction forces, and bilateral hip, knee, and ankle angles) and their derivatives to a 16-dimension state space. We build a linearly weighted regression model, \bar{q} , using data from multiple cycles to form a closed curve in this 16D state space. This curve is divided into 100 sections and labeled linearly with time. λ^* is the label of the nearest neighbor on the curve to the current measurement vector, as in [19].

At time t the sensors return an 16-element vector $\mathbf{q}(t)$. We compare this vector to the regression model \bar{q} . The state λ^* at time t is defined as

$$\lambda^*(t) = \arg \min_{\lambda \in [0, 100]} \|\mathbf{q}(t) - \bar{q}(\lambda)\|_2$$

Figure 4 illustrates how normalizing the data by λ^* aligns sensor measurements across different trials better than by time or percent gait cycle.

TABLE I
EVENT DETECTION ERROR RESULTS FOR EACH TECHNIQUE DUE TO SPEED AND ACTUATION PERTURBATION
EFFECTS FOR HEALTHY AND IMPAIRED SUBJECTS

5 Healthy Subjects					Impaired Subject				
Actuation Speed	Method	RMS Error (ms)	Ave. Error (ms)	Worst (ms)	Actuation Speed	Method	RMS Error (ms)	Ave. Error (ms)	Worst (ms)
Opsi Normal	CC	14.8±4.8	-1.7±2.9	35.5±19.1	Opsi Normal	CC	36.8	-3.6	76.7
	FT	14.8±5.6	1.7±1.5	30.5±9.7		FT	53.2	-1.4	138.2
	kNN	65.0±29.0	-14.8±9.6	208.1±194.3		kNN	104.6	-1.4	441.6
	λ*	6.4±1.2	-1.2±2.0	14.7±3.0		λ*	19.0	-6.2	33.3
	DE†	5.8±2.8	2.3±2.0	13.2±6.8		DE†	39.1	3.0	78.2
110psi Normal	CC	45.9±15.0	17.0±36.7	113.8±54.8	110psi Normal	CC	87.6	-64.2	23.4
	FT	41.9±11.8	27.6±15.3	106.5±52.4		FT	113.4	-86.0	44.1
	kNN	93.6±38.0	1.2±26.4	307.0±184.2		kNN	353.2	-25.1	762.9
	λ*	7.6±1.4	-0.9±2.6	18.7±5.6		λ*	15.5	0.5	57.4
	DE†	31.3±13.2	13.3±11.9	77.2±66.4		DE†	51.3	-25.8	19.2
Opsi Slow	CC	49.4±23.9	-29.0±25.2	37.7±26.1	Opsi Slow	CC	74.8	-47.2	62.3
	FT	69.6±15.7	-41.8±15.9	49.7±32.2		FT	108.8	-33.8	157.9
	kNN	77.8±32.4	10.8±18.9	289.7±199.0		kNN	110.9	-5.3	576.3
	λ*	9.5±4.2	0.3±2.7	30.4±28.5		λ*	18.4	-0.5	30.6
	DE†	14.2±5.1	-0.9±5.2	25.3±28.6		DE†	47.9	-8.6	78.0
110psi Slow	CC	84.0±53.2	-51.5±52.9	47.7±24.6	110psi Slow	CC	105.5	-81.1	21.5
	FT	82.9±20.9	-35.0±24.0	81.2±30.1		FT	175.7	-103.5	167.6
	kNN	112.7±88.7	3.9±27.2	272.0±190.9		kNN	214.8	17.2	681.9
	λ*	16.0±18.5	7.3±13.4	33.3±29.8		λ*	14.2	2.3	59.3
	DE†	37.9±12.6	5.9±15.5	59.8±22.4		DE†	50.2	-19.4	67.6

†The direct event detector (DE) can only detect toe off and heel strike on the right foot.

True event times for left and right heel strike and toe off events are detected using treadmill force sensors. **Gait period $T = 1.16 \pm 0.09s$ for healthy and $1.09 \pm 0.04s$ for impaired.** For the healthy subjects, errors are reported as mean±1 standard deviation. The best PPAFO estimator for each case is bolded and highlighted in dark gray. DE and the reference estimate λ* are highlighted in light gray and were not included in this comparison between estimators.

TABLE II
STATE ESTIMATION ERROR RESULTS FOR EACH TECHNIQUE DUE TO SPEED AND ACTUATION PERTURBATION
EFFECTS FOR HEALTHY AND IMPAIRED SUBJECTS

5 Healthy Subjects					Impaired Subject				
Actuation Speed	Method	RMS Error (λ)	Ave. Error (λ)	Worst (λ)	Actuation Speed	Method	RMS Error (λ)	Ave. Error (λ)	Worst (λ)
Opsi Normal	CC	1.3±0.4	-0.1±0.1	4.5±1.2	Opsi Normal	CC	2.9	0.4	7.7
	FT	1.3±0.5	-0.0±0.3	4.7±1.7		FT	4.3	1.5	11.4
	kNN	6.2±1.0	0.2±0.5	34.4±9.1		kNN	12.9	-2.4	49.4
110psi Normal	CC	3.5±1.6	-1.1±3.5	7.9±1.9	110psi Normal	CC	8.0	7.1	18.9
	FT	3.2±0.8	-1.5±1.6	9.7±2.4		FT	12.4	11.8	25.8
	kNN	8.9±2.0	0.2±2.2	41.3±9.4		kNN	21.6	6.1	49.0
Opsi Slow	CC	3.9±1.8	2.8±2.1	13.2±8.3	Opsi Slow	CC	7.1	6.2	14.6
	FT	7.7±1.7	6.4±1.5	18.1±3.6		FT	10.0	8.2	26.4
	kNN	8.5±1.1	-2.6±1.5	37.8±7.3		kNN	10.8	-0.5	48.0
110psi Slow	CC	7.1±3.7	5.6±4.3	13.9±5.6	110psi Slow	CC	9.6	8.4	19.9
	FT	9.3±3.6	7.4±3.2	21.3±6.3		FT	15.7	13.7	32.0
	kNN	8.2±3.5	-0.0±1.3	25.7±13.8		kNN	15.6	-1.9	51.5

For the healthy subjects, errors are reported as mean±1 standard deviation. The best estimator for each case is highlighted. Errors are the difference between PPAFO estimators and reference estimation λ*.

IV. RESULTS

CC and FT outperformed kNN for all tests. For the impaired subject, CC demonstrated the best accuracy for all tests, reducing event detection RMS error by up to 40% compared to FT. For the healthy subjects, FT and CC performed comparably during normal speed walking, but CC was more accurate during slow walking tests (Tables I and II).

1) *Normal Speed – No Actuation (Healthy and Impaired)*: For the healthy subject, both CC and FT worked well for event detection and state estimation, while kNN did not. **FT had low state estimate error around heel strike, but the error**

increased as time progressed in the gait cycle (Figure 5A) while CC stayed relatively low. For the impaired walker, the CC technique had a smaller average error (Figure 5B and 6). The FT estimate diverged more during swing (Figure 5B).

2) *Normal Speed – Actuation (Healthy and Impaired)*: This task verified that FT and CC can successfully track the system state, even when actuated. **The RMS error for state estimate is under 4% for the healthy subjects and around 10% for the impaired subject.** For the healthy subjects, FT and CC have similar performance, with FT having slightly higher accuracy. CC for the impaired subject has 23% lower RMS error than

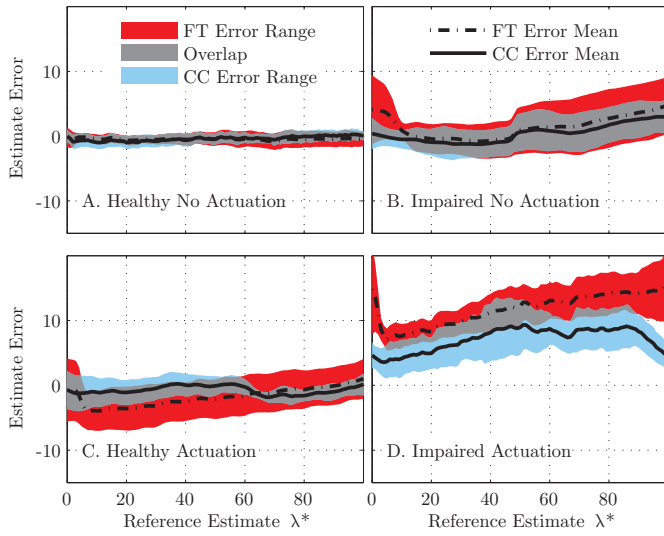


Fig. 5. Continuous state estimate error (mean and ± 1 standard deviation) of FT and CC estimators and the overlap of the two behaviors for healthy subject #3 and the impaired subject, with and without actuation.

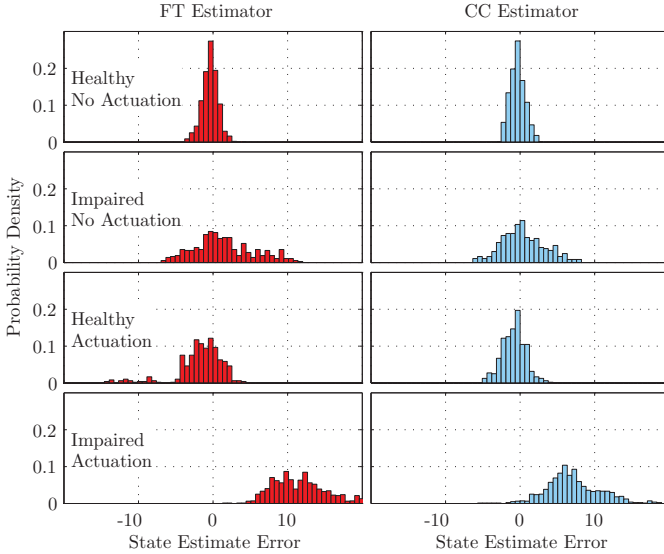


Fig. 6. Histograms of errors from FT and CC estimators for healthy subject #3 and the impaired subject, with and without actuation. The CC estimator demonstrates higher precision and often lower error, i.e., tighter distributions.

FT, a decrease in RMS state error from 12.4 to 8.0 (Table II).

3) *Slow Speed – No Actuation (Healthy and Impaired)*: For the healthy subjects, this test shows the largest improvements of CC over FT in both event detection and state estimate error. For both healthy and impaired subjects, the CC reduced the state estimate error by at least 29%, from 10 to 7.1 and the event detection error by at least 30%, from 69.6 to 49.4ms (Tables I and II).

4) *Slow Speed – Actuation (Healthy and Impaired)*: The combined speed and actuation perturbations make this the only test where k NN becomes competitive with other estimators. The healthy subjects were best estimated using CC. For the healthy subjects the state estimate RMS error was reduced 25% from FT to CC. For the impaired subject the results are

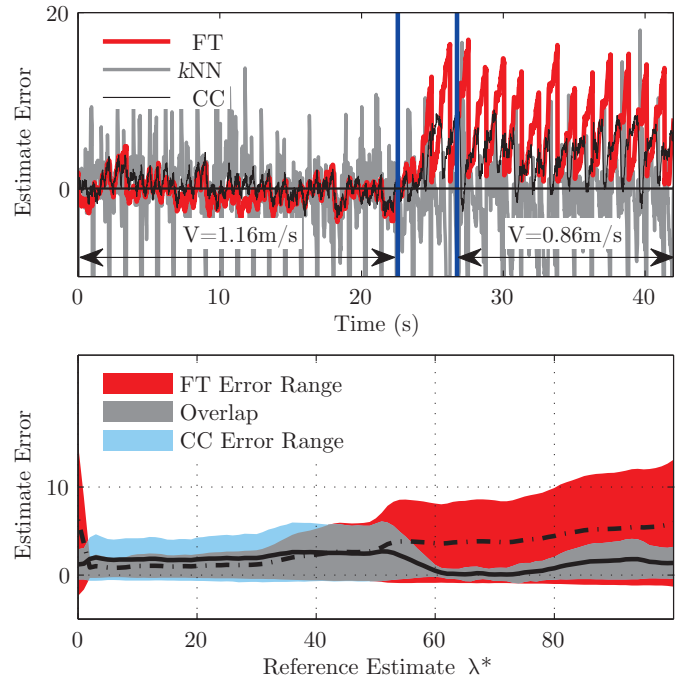


Fig. 7. Estimation error of healthy subject #3 during the change in speed test. The walking speed changed from 1.16m/s to 0.86m/s. Top: estimate error as a function of time. Bottom: overall estimate error as a function of state during the slow speed section. Note the high variance in the FT error at the slower speed caused by the cycle period T increasing from 1.16 ± 0.09 s to 1.32 ± 0.09 s.

striking: a 40% reduction in state estimate error from FT to CC, from 15.7 to 9.6 (Table II).

5) *Change in Speed (Healthy)*: This test reduced the walking speed by 25% midway through the trial. Figure 7 shows the errors from the three estimators as a function of overall time for this test. The error variance for FT illustrates unreliability at the slower walking speed, while CC maintains accuracy. The RMS and worst case for FT were all reduced by a factor of 2 by the CC estimate.

V. DISCUSSION

We have presented a new method of state estimation for powered PPAFOs (CC) that can be used to detect gait events. We also presented results from testing this method and three others (FT, k NN, and DE) in experimental trials during treadmill walking with both healthy and impaired subjects. In this section we will discuss the performance, robustness, applications to control, and limitations of these state estimation schemes.

A. Performance During Healthy Unperturbed Gait

The CC and FT estimators performed comparably during the healthy subject normal speed walking trials. The CC estimator correlates a window of past sensor readings to a regression model of normative sensor data to estimate the state. The FT estimator is an extension of the direct event (DE) estimator using thresholds, and only requires a model of the subject's

gait period. The FT has the advantage of simple implementation, but as we will discuss below, the CC estimator was more robust to disturbances.

The k NN estimator performed poorly during all subject trials. This estimator is based on [19], but uses PPAFO sensor data rather than motion capture data as in [19]. The poor performance of k NN was due to the limited data used to construct the subject's state configuration, and that k NN only makes use of the current sensor measurements. This shortcoming is compounded because the PPAFO sensor data contain large sections with nearly identical readings (Figure 2, e.g., 70-100% gait cycle). As a result, k NN cannot reliably compute gait state during these periods.

B. Robustness To Speed and Actuation Disturbances

The robustness of the estimators was evaluated during trials with speed and actuation disturbances. A decrease in speed was used to perturb gait because preliminary experimentation demonstrated greater estimation errors after a decrease rather than an increase in speed. Future work could examine the robustness of the CC estimator by applying time varying disturbances such as sinusoidal speed variations, accelerations/decelerations and gait initiation/cessation. A simple decision rule, rather than using the state estimators, was used to determine the timing of the actuation disturbance to allow for an unbiased comparison. This approach enabled the performance of the individual estimation schemes to be evaluated in the presence of the same disturbances. Our use of the term "actuation disturbance" may seem unusual, since the nominal purpose of the PPAFO is to provide assistance with applied torque. However, by choosing to view applied torque as a disturbance, we are hoping to ensure that estimators perform well regardless of the control policy used.

On average, the speed disturbance increased estimation error by a factor of 2.4 for healthy subjects and 1.9 for the impaired subject, and the actuation disturbance increased error by a factor of 2.6 for healthy subjects and 1.6 for the impaired subject.

The CC estimator was more robust to the speed perturbation and performed better during the impaired walking trials (both with and without actuation) as compared to the FT and k NN estimator (Tables I and II). The performance of FT and CC estimators were comparable during healthy walking trials perturbed by actuation. The k NN estimator was not robust to either of the disturbances.

The CC estimator performed well during all of the perturbed walking trials. The results from the impaired subject are particularly noteworthy because these results are representative of the intended population for this assistive device. During both perturbed and unperturbed gait of the impaired subject, the CC estimator outperformed the FT estimator by a minimum state estimation RMS error of 29% and a minimum event detection error of 23% (Tables I and II). The benefits of the CC estimator are also highlighted by the healthy walking trials with the speed perturbation, where the state estimate RMS error and event detection RMS error were up to 49% and 29% smaller than the errors resulting from the FT estimation. During the healthy walking trials with the actuation perturbation,

the performance of the CC estimator was comparable to the FT estimator. Actuation perturbation introduced differences to the sensor readings with little change to the cycle period (T for 0psi Normal: 1.16 ± 0.09 s vs. 110psi Normal: 1.18 ± 0.04 s). As a result, the FT estimator maintained accuracy, while the CC estimator was adversely affected by the weaker correlation between sensor measurements and the sensor regression models, Figures 3 and 5.

While the FT estimate performed well with the healthy walkers during normal speed walking and with actuation perturbation, this estimator was not robust to the speed perturbation. Figure 7 clearly shows the degradation in performance of the estimator following the decrease in speed. The speed perturbation changed the cycle period, leading to a reduction in FT estimator performance because FT was dependent on a predetermined cycle period. The FT estimator did not outperform the CC estimator during any impaired walking trials.

Table I shows that direct event detection (DE) RMS error was up to 6 times larger for the impaired subject than the healthy subjects during the normal walking trials. The increased event detection error is a significant component in the degradation of FT estimator performance for all impaired walking trials. Certain impaired walking patterns make event detection difficult, causing the DE estimator and any estimator relying on DE to perform poorly. In contrast, CC bases its estimate on the raw sensor measurements, not an assumed model of gait and thus is more robust to gait impairments.

C. Applications to Control

As we have emphasized throughout this paper, many powered AFOs rely on gait events to determine control objectives [9]–[18], and so reliable event detection is required for system control. Notable exceptions are powered orthotic systems that use surface EMG to directly control actuation [26]. That approach eliminates the necessity of gait event detection, but is limited by surface EMG signal reliability and availability.

In the current study, we have demonstrated that the CC estimator is able to accurately and robustly determine events during the gait cycle using data from PPAFO sensors. However, the CC estimator has broader applicability than just the PPAFO. In particular, a similar approach could be applied to provide state estimates for the control of any other assistive device (e.g., another orthosis or prosthesis) that has quasi-periodic inputs and outputs.

As we discussed in Section I, the control problem for an AFO has two parts, gait event detection and the controlled application of torque to meet the functional objective determined by each gait event. Our experiments showed the results (Tables I and II) of using state estimators to detect gait events but did not use these detected events as the basis for controlling torque. Future work will evaluate PPAFO performance during walking trials when state estimates (in particular, those provided by CC or FT) are used to control the actuation timing.

D. Current Limitations

The key limitation of our current approach to state es-

timation is that it requires a preliminary training process. This process was necessary to construct models used for state estimation. Inaccuracies in the CC estimate were created by mismatched training and actual testing conditions. One approach to reduce these inaccuracies would be to parameterize the models with respect to other gait variables such as gait period T . In this scenario, gait period would be measured directly from one of the sensors (e.g., heel sensor) and used to select the appropriate model from a library of predetermined models in real time. The training process was also time consuming and could serve as an impediment for use in a clinical setting. This issue could be addressed by continuously updating the regression model during gait. Such an approach could allow the system to adapt to changing environments, reduce the amount of training required to build the models, and improve session to session robustness since the models would be constructed as the subject walked.

The key limitation of our experimental study was that we only examined estimator performance during steady state, level walking on a treadmill in the gait lab. In order to successfully implement the estimation techniques outside of the lab, modes such as overground walking, ramp walking and stair ascent/descent must also be addressed. One approach would be to generate individual models for each mode and apply a methodology to switch between them. We will address these issues in future work.

VI. CONCLUSION

Accurate state estimates allow a powered AFO to adapt to changing environmental and functional needs. In contrast to previous methods of state estimation that rely largely on thresholding sensor measurements, this paper presented a method of state estimation based on cross-correlation between a window of past sensor measurements and a learned model. This approach—along with three others for comparison—was implemented on a powered AFO. Experiments with healthy and impaired subjects suggested that our cross-correlation state estimator provided the best overall performance.

ACKNOWLEDGMENT

This work was supported by the NSF Engineering Research Center for Compact and Efficient Fluid Power grant #0540834 and by NSF CAREER grant #0955088. The authors thank Emily Morris and the investigators in the Comparative Neuro-mechanics Laboratory at Georgia Tech (Prof. Young-Hui Chang, Megan Toney, and Jasper Yen) for their assistance.

REFERENCES

- [1] J. Perry, *Gait analysis: normal and pathological function*. Thorofare, NJ: Slack Inc., 1992.
- [2] R. R. Neptune, S. A. Kautz, and F. E. Zajac, "Contributions of the individual ankle plantar flexors to support, forward progression and swing initiation during walking," *J Biomech*, vol. 34, no. 11, pp. 1387–1398, 11 2001.
- [3] D. A. Winter, *Biomechanics and Motor Control of Human Movement*. Hoboken, New Jersey: John Wiley & Sons, Inc, 2005.
- [4] A. M. Dollar and H. Herr, "Lower extremity exoskeletons and active orthoses: Challenges and state-of-the-art," *IEEE Trans. Robot.*, vol. 24, no. 1, pp. 144–158, Feb. 2008.
- [5] T. M. Becker Orthopedic, "Becker orthopedic," Online Catalog.
- [6] S. Yamamoto, M. Ebina, M. Iwasaki, S. Kubo, H. Kawai, and T. Hayashi, "Comparative study of mechanical characteristics of plastic AFOs," *J Prosthet Orthot*, vol. 5, no. 2, 1993.
- [7] H. B. Kitaoka, X. M. Crevoisier, K. Harbst, D. Hansen, B. Kotajarvi, and K. Kaufman, "The effect of custom-made braces for the ankle and hindfoot on ankle and foot kinematics and ground reaction forces," *Arch Phys Med Rehabil*, vol. 87, no. 1, pp. 130–135, 2006.
- [8] G. K. Rose, *Orthotics: Principles and Practice*. London: Williams Heinemann., 1986.
- [9] W. Svensson and U. Holmberg, "Ankle-foot-orthosis control in inclinations and stairs," *IEEE Conf on Robotics, Automation and Mechatronics*, pp. 301–306, 2008.
- [10] J. A. Blaya and H. Herr, "Adaptive control of a variable-impedance ankle-foot orthosis to assist drop-foot gait," *IEEE Trans. Neural Syst. Rehabil. Eng.*, vol. 12, no. 1, pp. 24–31, 2004.
- [11] A. W. Boehler, K. W. Hollander, T. G. Sugar, and D. Shin, "Design, implementation and test results of a robust control method for a powered ankle foot orthosis (AFO)," *ICRA*, pp. 2025–2030, 2008.
- [12] J. Furusho, T. Kikuchi, M. Tokuda, T. Kakehashi, K. Ikeda, S. Morimoto, Y. Hashimoto, H. Tomiyama, A. Nakagawa, and Y. Akazawa, "Development of shear type compact MR brake for the intelligent ankle-foot orthosis and its control," *ICORR*, pp. 89–94, 2007.
- [13] C. M. Kim and J. J. Eng, "The relationship of lower-extremity muscle torque to locomotor performance in people with stroke," *Phys Ther*, vol. 83, no. 1, pp. 49–57, 2003.
- [14] D. J. Weber, R. B. Stein, K. M. Chan, G. Loeb, F. Richmond, R. Rolf, K. James, and S. L. Chong, "Bionic walkaide for correcting foot drop," *IEEE Trans. Neural Syst. Rehabil. Eng.*, vol. 13, no. 2, pp. 242–246, June 2005.
- [15] K. W. Hollander, R. Ilg, T. G. Sugar, and D. Herring, "An efficient robotic tendon for gait assistance," *J Biomech Eng*, vol. 128, no. 5, pp. 788–791, 2006.
- [16] J. Hitt, A. M. Oymagil, T. Sugar, K. Hollander, A. Boehler, and J. Fleeger, "Dynamically controlled ankle-foot orthosis (DCO) with regenerative kinetics: Incrementally attaining user portability," *ICRA*, pp. 1541–1546, 10-14 April 2007.
- [17] J. M. Hausdorff and H. Ring, "Effects of a new radio frequency-controlled neuroprosthesis on gait symmetry and rhythmicity in patients with chronic hemiparesis," *Am J Phys Med Rehabil*, vol. 87, no. 1, pp. 4–13, 2008.
- [18] K. A. Shorter, E. T. Hsiao-Weckslar, G. F. Kogler, E. Loth, and W. K. Durfee, "A portable-powered-ankle-foot-orthosis for rehabilitation," *J Rehabil R D*, accepted 2010.
- [19] A. Forner-Cordero, H. J. F. M. Koopman, and F. C. T. van der Helm, "Describing gait as a sequence of states," *J Biomech*, vol. 39, no. 5, pp. 948–957, 2006.
- [20] R. W. Oppenheim, A. V. S., *Digital Signal Processing*. Upper Saddle River, New Jersey: Prentice Hall, 1975.
- [21] R. T. Collins, R. Gross, and J. Shi, "Silhouette-based human identification from body shape and gait," *IEEE Conf on Automatic Face and Gesture Recognition*, pp. 366–371, 2002.
- [22] J. Mantyjarvi, M. Lindholm, E. Vildjiounaite, S. M. Makela, and H. A. Ailisto, "Identifying users of portable devices from gait pattern with accelerometers," *ICASSP '05*, vol. 2, pp. 973–976, 2005.
- [23] R. Kram, T. M. Griffin, J. M. Donelan, and Y. H. Chang, "Force treadmill for measuring vertical and horizontal ground reaction forces," *J Appl Physiol*, vol. 85, no. 2, pp. 764–769, 1998.
- [24] W. S. Cleveland and S. J. Devlin, "Locally weighted regression: An approach to regression analysis by local fitting," *J Am Stat Assoc*, vol. 83, no. 403, pp. 596–610, 1988.
- [25] C. M. Bishop, *Pattern Recognition and Machine Learning*. Springer, 2006.
- [26] D. P. Ferris, K. E. Gordon, G. S. Sawicki, and A. Peethambaran, "An improved powered ankle-foot orthosis using proportional myoelectric control," *Gait & Posture*, vol. 23, no. 4, pp. 425–428, 2006.